Published in final edited form as:
Circ Res. 2014 June 20; 115(1): 10–22. doi:10.1161/CIRCRESAHA.115.303100.

Control of Very-Low Density Lipoprotein Secretion by N-Ethylmaleimide-Sensitive Factor and miR-33

Ryan M. Allen, **Tyler J. Marquart**, **Jordan J. Jesse**, and **Ángel Baldán**
Edward A. Doisy Department of Biochemistry & Molecular Biology, and Center for Cardiovascular Research, Saint Louis University, Saint Louis, MO

Abstract

Rationale—Several reports suggest that antisense oligonucleotides against miR-33 might reduce cardiovascular risk in patients by accelerating the reverse cholesterol transport pathway. However, conflicting reports exist regarding the impact of anti-miR-33 therapy on the levels of very low-density lipoprotein-triglycerides (VLDL-TAG).

Objective—We test the hypothesis that miR-33 controls hepatic VLDL-TAG secretion.

Methods and Results—Using therapeutic silencing of miR-33 and adenoviral overexpression of miR-33, we show that miR-33 limits hepatic secretion of VLDL-TAG by targeting N-ethylmaleimide-sensitive factor (NSF), both in vivo and in primary hepatocytes. We identify conserved sequences in the 3'UTR of *NSF* as miR-33 responsive elements, and show that *Nsf* is specifically recruited to the RNA-Induced Silencing Complex (RISC) following induction of miR-33. In pulse-chase experiments, either miR-33 overexpression or knock-down of *Nsf* lead to decreased secretion of apoproteins and TAG in primary hepatocytes, compared to control cells. Importantly, *Nsf* rescues miR-33–dependent reduced secretion. Finally, we show that overexpression of *Nsf* in vivo increases global hepatic secretion and raises plasma VLDL-TAG.

Conclusion—Together, our data reveal key roles for the miR-33–NSF axis during hepatic secretion, and suggest that caution should be taken with anti-miR-33–based therapies since they might raise pro-atherogenic VLDL-TAG levels.

Keywords

miR-33; VLDL; triglycerides; secretion; miR; lipoprotein; liver; N-ethylmaleimide-sensitive factor

INTRODUCTION

VLDL (very low-density lipoproteins) are triacylglyceride-rich lipoproteins synthesized in the liver. Following secretion, the triacylglyceride (TAG) core of VLDL is metabolized in

Address Correspondence to: Dr. Ángel Baldán, Department of Biochemistry & Molecular Biology, Doisy Research Center, room 427, Saint Louis University, 1100 S. Grand Blvd., Saint Louis, MO 63104, Tel: +1-314-977-9227, Fax: +1-314-977-9206, abaldan1@slu.edu.

DISCLOSURES
R.M.A., T.J.M., and Á.B. are pursuing a patent related to miR-33. J.J.J. has no conflicts of interest.

peripheral tissues by lipoprotein lipase, rendering cholesteryl ester-rich LDL (low-density lipoproteins) that can accumulate in the arterial sub-endothelial spaces and trigger the development of atherosclerosis. The biogenesis of VLDL begins with the MTTP (microsomal triglyceride transfer protein)-dependent lipidation of APOB in the ER (endoplasmic reticulum) of the hepatocyte (reviewed in[1, 2]). Nascent lipoprotein-containing vesicles are then trafficked from the ER to the Golgi, where APOB is glycosylated and phosphorylated, and eventually to the plasma membrane for secretion into the sinusoidal space and release into the circulation. The trafficking of VLDL from ER to Golgi has been particularly well studied, and we now know that APOB-containing vesicles are quite different from other protein-containing vesicles budding out of the ER, not only in cargo but also in coating proteins. Hence, the Fisher and Siddiqi groups showed that efficient vesicular transport of VLDL out of the ER requires not only the COPII (coat complex II) machinery, but also the presence of the v-SNARE (vesicle-N-ethylmaleimide-sensitive factor-attachment protein receptor) SEC22B, which is recognized in the Golgi by the t-SNAREs (target-SNAREs) STX5, BET1, and GOSR1[3-5]. The binding of v- and t-SNAREs to form the so-called cis-SNARE complex is one of the hallmarks of directional vesicular trafficking, allowing vesicle and target membranes to come in close proximity thus facilitating membrane fusion and the release of the cargo into the lumen of the target compartment (reviewed in[6]). The cis-SNARE complexes are eventually resolved by the hexameric ATPase NSF (N-ethylmaleimide-sensitive factor), which is recruited to the SNARE complex by the adaptor protein SNAP (soluble NSF-attachment protein)[6]. Whether NSF activity is also required for membrane fusion is still much debated. Nevertheless, data suggest that disruption of NSF activity alters intracellular vesicular trafficking and prevents normal secretion in a variety of cells[6].

MicroRNAs (miRNA) are small, ~22 nt RNA molecules that associate to the RNA-Induced Silencing Complex (RISC) and modulate the expression of target mRNA by binding to complementary sequences (generally in the 3'UTR) and subsequently promoting translational suppression and/or RNA degradation[7]. In the last decade, miRNA have been recognized as essential regulators of multiple (patho)physiological processes. We and others have reported on miR-33 (also known as miR-33a or miR-33a-5p): an intragenic miRNA encoded within intron 16 of SREBP-2 that controls the expression of several transmembrane sterol transporters that include ABCA1, ABCG1, NPC1, ABCB11 and ATP8B1[8-13]. Early reports using miR-33$^{-/-}$ mice[12] or mice where miR-33 expression was silenced with antisense oligonucleotides[8-10, 13, 14] showed increased circulating HDL-cholesterol and/or bile secretion. Importantly, non-human primates also exhibited increased HDL-cholesterol levels following treatment with anti-miR-33 oligonucleotides[15, 16]. Consistent with these data, silencing of anti-miR-33 led to increased reverse cholesterol transport (RCT) in vivo in both wild type[13] and atherosclerosis-prone *Ldlr*$^{-/-}$[14] mice, compared to control oligonucleotides. The RCT pathway mobilizes extrahepatic cholesterol into HDL back to the liver, where it is metabolized to bile acids and subsequently secreted into the bile for final excretion through the feces. Thus, RCT is regarded as atheroprotective and strategies that promote/accelerate the flow of cholesterol through this pathway are predicted to be effective in reducing the risk of cardiovascular disease in patients[17]. These reports suggested that silencing of hepatic miR-33 expression (e.g. anti-miR-33 oligonucleotides) might reduce

cardiovascular risk in patients. However, we and others have reported conflicting results after therapeutic silencing of miR-33 in *Ldlr*$^{-/-}$ mice[14, 18, 19].

Herein we show that prolonged silencing of miR-33 results in a sustained raise in hepatic secretion, leading to increased plasma levels of VLDL-TAG and other liver-secreted proteins in chow-fed C57BL/6 mice, compared to animals treated with saline or control oligonucleotides. Using mouse primary hepatocytes, we demonstrate that *Nsf* is recruited to the RISC following miR-33 overexpression, and that NSF mediates miR-33–dependent changes in secretion. Finally, we show that manipulation of hepatic NSF levels in vivo results in changes in hepatic secretion, including changes in plasma VLDL-TAG. Collectively, our data uncover NSF as a key regulator of hepatic secretion, and suggest a role for miR-33 on intracellular vesicular trafficking.

METHODS

Male 12 week-old C57BL/6 mice (NCI–Charles River Laboratories) were maintained on a 12h/12h light/dark cycle with unlimited access to food and water. Where indicated, mice were injected i.p. with 200 μL saline, or 5 mg/Kg control (5'-TCCTAGAAAGAGTAGA) or anti-miR-33 (5'-TAGCAACTACAATAGCA) oligonucleotides (a kind gift from Miragen Therapeutics, Inc) once a week. Other animals were infused via tail vein with empty or NSF adenoviral vectors (2×10^9 pfu). Mouse cohorts are described in Online Table I. All animal studies were reviewed and approved by the IACUC at Saint Louis University.

Detailed Methods are provided as online Supplemental Material.

RESULTS

Long-term silencing of miR-33 raises plasma VLDL-TAG in chow-fed mice

To gain insight into the physiological consequences of long-term silencing of miR-33 expression, we dosed chow-fed C57BL/6 mice i.p. with saline, or control or anti-miR-33 oligonucleotides (5 mg/Kg) once per week for 11 weeks. We did not observe significant changes in body weight gain among the different groups (Online Figure IA). Consistent with our reported data in WD-fed *Ldlr*$^{-/-}$ mice[19], mice receiving anti-miR-33 oligonucleotides showed sustained elevated plasma TAG levels, compared to control animals (Figure 1A). TAG lipoprotein profiles of pooled plasma samples at weeks 3 and 11 (Figure 1B), and western blot analysis of plasma APOB100 at week 11 (Figure 1C) were consistent with an increase in circulating VLDL-TAG in mice dosed with anti-miR-33, compared to controls. The levels of circulating APOB48, however, remained unchanged between groups. Plasma cholesterol levels increased, as expected, in the anti-miR-33 group for the first 5 weeks, but returned to normal thereafter (Online Figure IB). Analysis of the livers showed a ~70% drop in miR-33 levels (Figure 1D), and a concomitant induction of known miR-33 targets (i.e. ABCA1, CPT1A) at both the mRNA (Online Figure ID) and protein (Figure 1E) levels in animals receiving anti-miR-33 treatment, compared to controls. As described previously[13, 15, 19], the anti-miR-33 treatment resulted in a significant decrease in the amounts of hepatic FASN (Figure 1E and Online Figure ID). Data also show that at the mRNA level, both *Mttp* and *Apob* were modestly induced in the anti-miR-33 group,

compared to controls (Online Figure ID). However, no significant changes were noted at the protein levels for MTTP and APOB48 between treatments (Figure 1E). The levels of APOB100, in contrast, were modestly increased in the livers of the anti-miR-33 group, compared to controls (Figure 1E). Finally, analysis of hepatic lipid contents revealed a significant increase in the amounts cholesteryl esters in mice receiving anti-miR-33, compared to controls (Online Figure IE), but no changes in TAG, non-esterified fatty acids or cholesterol, or phosphatidylcholine (Online Figure IE). Collectively, data in Figure 1 and Online Figure I suggest that prolonged silencing of miR-33 using oligonucleotides in chow-fed mice results in elevated VLDL-TAG and APOB100 in circulation.

MiR-33 limits hepatic VLDL secretion in vivo

We hypothesized that the changes in circulating TAG in the anti-miR-33 treatment group might be the result of accelerated hepatic VLDL secretion. To test this proposal, we measured hepatic TAG secretion in vivo in a second cohort of mice using the tyloxapol method (see Experimental Procedures). Briefly, six weeks into the treatment with saline, or control or anti-miR-33 oligonucleotides, mice were fasted overnight and then injected i.v. with tyloxapol, which inhibits lipoprotein lipase (LPL) activity and thus prevents the degradation of circulating TAG. Consequently, TAG accumulate in circulation over time in direct proportion to the rate of hepatic secretion. Data in Figure 2A show the kinetics of plasma TAG accumulation in the 3 groups of mice over 3 h. As expected, no changes in plasma TAG were noted between mice receiving saline or control oligonucleotides; in contrast, circulating TAG accumulated in the anti-miR-33 group at a significantly faster pace (Figure 2A). The actual secretion rates calculated from the slopes of the different curves demonstrated that depletion of miR-33 in the liver results in accelerated VLDL secretion, compared to controls (Figure 2B).

We next used mouse primary hepatocytes to further validate a role for miR-33 on VLDL secretion. Cells were transduced with an empty or miR-33-encoding adenovirus, pulsed with cold- or [^{14}C]-oleate, and chased for 24 h in fresh media. As expected, miR-33 overexpression resulted in decreased mRNA levels of known targets (data not shown). Consistent with a role for miR-33 on VLDL secretion, we noted both reduced amounts of APOB100 and APOB48 (Figure 2C) and reduced radioactivity (Figure 2D) in supernatants recovered from cells overexpressing miR-33, compared to control cells. Intriguingly, the levels of APOA1 were also diminished in the supernatants from cells overexpressing miR-33 (Figure 2C). Lipids extracted from both the media and the cells were resolved by thin layer chromatography along with standards for different classes of lipids. Data show that the amounts of [^{14}C]-labeled TAG, DG, and FFA, but not PL, were significantly reduced in the supernatants from cells overexpressing miR-33, compared to control cells (Figures 2E, G). Whether the DG and FFA in the media are actively secreted or the result of the hydrolysis of secreted TAG is unknown. Importantly, these changes in lipid secretion were not the result of decreased incorporation of [^{14}C]-oleate into different classes of lipids in cells overexpressing miR-33, since intracellular labeled lipids did not differ between control and miR-33 cells (Figure 2F, H). Additionally, the changes in lipid and APOB secretion in miR-33–overexpressing hepatocytes were not the result of altered de novo lipogenesis (DNL) or fatty acid β-oxidation (FAO) either, as measured by the incorporation

of [^{14}C]-acetate into different classes of lipids and the release of labeled water from [^{3}H]-palmitate, respectively: although no significant changes were noted, both parameters trended down in hepatocytes overexpressing miR-33, compared to control cells (Online Figure IIA–C). However, and consistent with a reduction in VLDL secretion, the levels of total intracellular TAG were modestly increased in cells overexpressing miR-33, compared to control cells (Online Figure IID); likewise, total intracellular cholesterol levels were elevated in the same cells (Online Figure IID), likely the result of reduced ABCA1 expression. Taken together, data from Figures 1 and 2 suggest that hepatic miR-33 modulates the secretion of VLDL-TAG both in vitro and in vivo.

APOB and MTTP are not direct miR-33 targets

Data in Figures 1 and Online Figure ID showing elevated APOB100 in circulation and moderately increased levels of *Apob* and *Mttp* following silencing of miR-33 are compatible with one or both of these genes being a direct target of the miRNA. That proposal would be consistent with the well-known role of these genes during VLDL biogenesis. Indeed, analysis of *APOB* and *MTTP* revealed the presence of conserved sequences that were partially complementary to miR-33 (Figure 3A, B). However, when cloned downstream of a luciferase reporter these sequences did not confer responsiveness to miR-33 in transient transfection experiments in HEK293 cells (Figure 3C, D). Additionally, the mRNA and protein levels of *APOB* and *MTTP* did not change in mouse primary hepatocytes or in human HuH7 cells following overexpression of miR-33, compared to control cells (Figure 3E, F). Collectively, these data suggest that neither *APOB* nor *MTTP* are direct targets of miR-33.

NSF is a direct, functional miR-33 target

We next turned our attention to genes encoding proteins involved in VLDL vesicular trafficking (see Introduction). First, we tested whether overexpression of miR-33 in either mouse primary hepatocytes or human HuH7 hepatoma cells could reduce the expression of any of such genes. Data in Figure 4A, B and Online Figure IIIA, B show that both the mRNA and protein levels of NSF are decreased in cells overexpressing miR-33, compared to controls. In contrast, the levels of *NAPA* (which encodes α-SNAP, the main SNAP expressed in the liver), *SEC22B*, *GOSR1*, *STX5*, or *BET1* remained unchanged between treatments. These data suggested that NSF could be a direct target of miR-33. To validate this proposal, we then tested whether the *Nsf* is actively recruited to the RISC following miR-33 overexpression. Mouse primary hepatocytes were transduced with empty or miR-33-encoding adenovirus, whole extracts prepared 48 h later, and the RISC complexes immunoprecipitated using an AGO2 (Argonaut-2) antibody (see Experimental Procedures). Known miR-33 targets (*Abca1*, *Atp8b1*, *Abcb11*, *Cpt1a*, and *Crot*) were selectively enriched in the RISC of miR-33 overexpressing cells, while at the same time decreased in total RNA, compared to controls (Figure 4C), thus proving the specificity of the experiment. Data from the same samples show that *Nsf* also meets the criteria of a bona-fide miR-33 target: recruitment to the RISC and decrease in transcriptome in miR-33 overexpressing hepatocytes (Figure 4C); in contrast, the other members of the SNARE pathway with a role on VLDL trafficking (*Napa*, *Sec22b*, *Gosr1*, *Stx5*, and *Bet1*), were not enriched in the RISC

and/or their expression did not change following miR-33 overexpression. These data strongly suggest that NSF is a direct target of miR-33.

Based on these results, we next sought to characterize the miR-33 responsive elements in *NSF*. The miRNA target prediction algorithm Targetscan identified three conserved sequences in the 3'UTR of mouse and human *NSF* that are partially complementary to miR-33 (sites 1–3 in Figure 4D). Interestingly, elements 2 and 3 are partially overlapping, similar to the miR-33 elements in ABCA1[8-12]. These sequences, or the entire 3'UTR of mouse or human *NSF*, were cloned downstream of a luciferase reporter, and transiently transfected into HEK293 cells in the presence or absence of a plasmid encoding miR-33. Data from these experiments show that the 3'UTR fragments and the cluster containing sites 2 and 3, but not site 1, were able to confer responsiveness to miR-33 (Figure 4E). Importantly, specific point mutations in elements 2 or 3 that prevent interaction with the seed sequence of miR-33 abrogated the response to the miRNA (Figure 4E). Together, these data identify sequences 2 and 3 as functional miR-33 responsive elements.

Finally, we checked the hepatic expression of NSF, NAPA, and selected v- and t-SNAREs in the livers of mice dosed with saline, or control or anti-miR-33 oligonucleotides (Figure 1). Consistent with the data shown above, NSF was increased both at the mRNA and protein levels in the livers of the anti-miR-33 group, compared to controls (Figures 4F and Online Figure IIIC). No significant changes were noted for the other genes studied, with the exception of a modest increase of *Stx5* at the mRNA but not protein level in anti-miR-33 treated livers (Figures 4F and Online Figure IIIC). Taken together, the in vivo and in vitro data shown in Figure 4 identifies NSF as a physiological target of miR-33.

NSF controls TAG and APOB secretion in primary hepatocytes

Based on the well-known role of NSF on intracellular vesicular trafficking, we hypothesized that miR-33-dependent changes in NSF expression may account for the altered secretion of VLDL-TAG in mice dosed with anti-miR-33 oligonucleotides (Figures 1A, B, and 2A, B). We therefore tested whether changes in NSF abundance modulate the secretion of TAG and/or APOB using antisense oligonucleotides to knock-down *Nsf* in mouse primary hepatocytes. By titrating the amounts of siRNA used, we aimed at mimicking the levels of NSF repression obtained when miR-33 was overexpressed (compare Figure 5A, B vs. Figure 4A, B). While this approach was successful in dose-dependently decreasing the protein levels of NSF, it did not affect the levels of intracellular MTTP or APOB (Figure 5B). At the mRNA level, however, we noted an increase in *Mttp* and a decrease in both β-oxidation genes (*Cpt1a, Acox*) and lipogenic genes (*Fasn, Acc, Scd1*) in samples transfected with anti-*Nsf* oligonucleotides, compared to controls (Online Figure IVA). Of critical significance for our hypothesis, the decrease in intracellular NSF in cells overexpressing miR-33 was paralleled by a dose-dependent reduction in APOB100, APOB48, and APOA1 recovered from the supernatants of the same cells, compared to controls (Figure 5C). Remarkably, we also observed a dose-dependent increase in intracellular APOA1 in the same cells (Figure 5B). Taken together, these data suggest that the changes in the amounts of apoproteins recovered in the media of cells with reduced NSF expression are not due to reduced protein synthesis, but rather to decreased secretion. The fact that APOB did not also accumulate in

the low-NSF expressing cells might be the consequence of constitutive ERAD-dependent degradation and/or autophagy of excess non-secreted APOB (reviewed in[20]).

In parallel experiments, we tested whether reduced NSF expression would also alter lipid secretion. Hence, following transfection with non-targeting or anti-*Nsf* siRNA, primary hepatocytes were pulsed with [^{14}C]-oleate and subsequently chased for 24 h in fresh medium. Data show that partial knock-down of NSF did not alter the ability of cells to incorporate the labeled fatty acid into different classes of lipids (Figure 5D, E), but led to decreased recovery of radiolabelled lipid species (TAG, DAG and FFA, but not PL) from the supernatants (Figure 5F, G), compared to control cells. These data are strikingly reminiscent of the results obtained following miR-33 overexpression in primary hepatocytes (Figure 2E–F), and suggest both that NSF activity is rate limiting for constitutive hepatic lipoprotein secretion and that NSF likely mediates miR-33-dependent changes in VLDL secretion.

NSF overexpression enhances TAG and APOB secretion, and rescues the effect of miR-33

To complement the knock-down studies shown above, we next performed overexpression experiments in which primary hepatocytes were transduced with either an empty adenovirus or an adenovirus encoding murine NSF. The next day, cells were washed and incubated in fresh media for an additional 24 h without supplementation of fatty acids. Importantly, under these conditions APOB secretion is typically very inefficient[21]. Our data show that MTTP protein levels did not change in cells overexpressing NSF, compared to control cells (Figure 6A), despite the significant increase in mRNA levels (Online Figure IVB). Meanwhile, the levels of APOB protein, but not mRNA, were slightly increased in the same cells, compared to controls (Figure 6A and Online Figure IVB). On the other hand, supernatants from cells transduced with the empty adenovirus contained very little APOB48/100 as determined by western blot (Figure 6B), as expected. In contrast, supernatants from cells transduced with the NSF adenovirus contained increased amounts of APOB100/48 and APOA1. These results are consistent with those from knock-down experiments above, and strongly suggest that NSF activity enhances lipoprotein secretion. Importantly, manipulation of NSF levels with either siRNA or adenovirus did not result in significant cell toxicity or death, as measured by LDH activity released to the supernatant, ability to cleave MTT, activation of caspase 3, or *Tnfα* expression (Online Figure IVC).

Next, to validate the role of NSF on hepatic VLDL secretion *in vivo* we transduced male C57BL/6 mice (n=5) with empty or NSF adenoviral vectors, via tail vein injection. After seven days, the animals were fasted overnight, euthanized, and liver and plasma samples collected. Using this approach NSF was efficiently overexpressed in mice receiving Adeno-*Nsf*, compared to controls (Figure 6C, D). Similar to data from primary hepatocytes, increased NSF levels was not paralleled by significant changes in the abundance of MTTP and APOB (Figure 6D), although *Mttp* levels were slightly increased in the same livers (Figure 6C). Importantly, plasma TAG levels, but not cholesterol, were significantly elevated in mice overexpressing NSF, compared to controls (Figure 6E, F). Consistent with these data, circulating APOB, but not APOA1, were also elevated in the same plasma samples (Figure 6G). To determine whether the changes in plasma TAG in NSF-

overexpressing mice were the consequence of enhanced VLDL secretion, we transduced an additional cohort of mice with empty or NSF adenoviral vectors (n=6), as above, and then measured hepatic TAG secretion using the tyloxapol method. Five days post-adenoviral transduction, mice were fasted overnight and blood samples were collected before and after an *i.v*. injection of tyloxapol (as described for Figure 2A). Data show a significantly faster accumulation of TAG in the plasmas of mice overexpressing NSF, compared to controls (Figure 6H), which translated into a ~30% increased hepatic secretion rate (Figure 6I). An additional experiment in a third cohort of mice (n=6) transduced with adenoviral vectors and used for tyloxapol experiments resulted in virtually identical results (Online Figure VA, B). Taken together, our studies both in primary hepatocytes and in vivo strongly suggest that changes in hepatic NSF expression alter VLDL-TAG secretion.

Finally, we tested whether NSF could rescue the miR-33–dependent decrease in TAG and APOB secretion. Primary hepatocytes were transduced with or without adenovirus encoding miR-33 and/or *Nsf* in media supplemented with 0.8 mmol/L oleate, then pulsed with [^{14}C]-oleate, and chased for 24 h in fresh medium. As expected, the secretion of APOB was higher in these cells, compared to those cultured in media without oleate supplementation (Figure 7B *vs*. 6B). Nevertheless, data in Figure 7A–D show that the secretion of both APOB and labeled TAG were decreased by miR-33 and increased by NSF, respectively. Importantly, NSF overexpression reverted the effects of miR-33 on both APOB and TAG secretion (Figure 7B, C) without altering the incorporation of [^{14}C] into intracellular lipid pools (Online Figure VI), suggesting that NSF mediates miR-33–dependent changes in VLDL secretion.

The miR-33–NSF axis controls the overall secretory pathway in primary hepatocytes

Since NSF is a universal ATPase required for the resolution of all cis-SNARE complexes, we next hypothesized that changes in the levels of miR-33 or NSF also alter the global pattern of secretion from the hepatocyte, which may account for the consistent changes in APOA1 secretion noted in previous figures. To test this proposal, we performed a [^{35}S]-Met/Cys pulse-chase experiment in primary mouse hepatocytes transduced with empty, miR-33 or NSF adenoviral vectors. Similar specific activities (i.e., dpm/μg protein) were recorded for intracellular protein extracts (Figure 7E), consistent with no changes in protein synthesis among the different treatments. However, the amounts of labeled proteins recovered from the supernatants were significantly decreased in cells overexpressing miR-33, and increased in cells overexpressing *Nsf*, compared to control cells (Figure 7F). Together, these data are consistent with an overall effect of miR-33 and NSF on secretion.

We next tested whether NSF could rescue the miR-33–dependent decrease in global secretion. Figure 7G provides a proof-of-concept experiment in human HuH7 hepatoma cells that were co-transfected with both intracellular (LUC) and constitutively secreted (GLUC) luciferase vectors, in the presence or absence of expression vectors for miR-33 and NSF. The GLUC and LUC activities were recorded in supernatants and cell extracts, respectively, over time (see Experimental Procedures). Data show that miR-33 significantly decreased the secretion of the GLUC, compared to basal conditions. Not only did NSF raise basal GLUC secretion but it also reversed the effect of miR-33 (Figure 7G). Importantly, the

changes in normalized media GLUC activity cannot be explained by changes in *Gluc* expression, since similar mRNA levels were noted among the different treatments (Figure 7G, insert). These *in vitro* results provide decisive evidence for our hypothesis that the miR-33–NSF axis regulates the overall secretory pathway in hepatocytes from both mice and humans.

Based on these data, we reasoned that global changes in hepatic secretion should also be observed in vivo following manipulation of miR-33 or NSF. Hence, we checked the levels of several proteins associated (APOB, APOA1, APOE, LCAT) or not (ALBUMIN, TRANSFERRIN, C3A) with lipoprotein metabolism in plasma samples from either mice treated with saline, scrambled or miR-33 oligonucleotides (Figure 8A), or mice transduced with empty or NSF adenoviral vectors (Figure 8B). In agreement with our hypothesis, samples from both anti-miR-33 and Adeno-*Nsf* treated mice showed higher titers for most, but not all, of the proteins studied. On the contrary, IgG, which is not secreted from the liver, remained unchanged among groups. A potential limitation of these in vivo data is that circulating levels of proteins are likely affected by a multiplicity of factors besides secretion, that include uptake in peripheral tissues, degradation, and renal clearance, and thus plasma levels may not directly reflect changes in hepatic output. To avoid this limitation, we performed new tyloxapol experiments in mice simultaneously injected with [^{35}S]-Met/Cys, thus allowing us to study the appearance in circulation of newly synthetized hepatic proteins. Data in Figure 8C, D and 8H, I show that either anti-miR-33 treatment or adenoviral mediated NSF overexpression resulted, again, in accelerated TAG accumulation in plasma, compared to control animals. Such rise in VLDL secretion was paralleled by the increased abundance of plasma [^{35}S]-labeled APOB, APOA1, and ALBUMIN in the same mice, compared to controls (Figure 8E–G and 8J–L). Taken together, data in Figure 8 support our proposal that miR-33 regulates global secretion in the hepatocyte by targeting NSF.

DISCUSSION

Impaired lipid homeostasis is generally recognized as a risk factor for the development of atherosclerosis, the primary cause of heart attack and stroke, which collectively account for ~32% of all deaths in the US[22]. The vast majority of dyslipidemic patients are prescribed statins, which act as competitive inhibitors of HMGCR, the rate-limiting enzyme in cholesterogenesis. The therapeutic benefit of statins is due, at least in part, to the increased maturation of SREBP-2, which then promotes the expression of the LDLR and thus the accelerated clearance of pro-atherogenic lipoproteins from circulation. Importantly, *SREBP-2* levels are also induced by statins, since SREBP-2 trans-activates its own promoter. We and others showed that conditions that promote SREBP-2 maturation (such as reduced intracellular contents, or treatment with statins) also raise the levels of its intragenic miR-33[8-10]. Therefore, from a clinical perspective it may be important that statins induce the expression of miR-33. Our data suggest that miR-33/NSF–dependent changes in VLDL secretion, together with the accelerated uptake of APOB-containing lipoproteins via the LDLR, may help explain the significant drop in plasma TAG noted in patients and animal models taking statins[23, 24]. Studies in patients using stable isotopes and radiolabeled lipoproteins to measure hepatic APOB secretion in response to statins have been mixed,

though: some authors reported decreased APOB secretion[25-29] while others found no changes[30-33].

However, caution must be taken when translating the results from anti-miR-33 studies from mice to humans. Primates, but not rodents, express a second copy of miR-33 from within an intron of *SREBP-1*. MiR-33a (co-transcribed with *SREBP-2*) and miR-33b (co-transcribed with *SREBP-1*) share the same seed sequence, but differ in 2 nucleotides in the 3' region. Whether these 2 nt confer target specificity remains to be determined. Nonetheless, the Moore and Temel groups showed that an oligonucleotide that is 100% complementary to miR-33a effectively reduces the functional levels of both miR-33a and miR-33b[15]. Importantly, the transcription of *SREBP-2* and *SREBP-1* is controlled by different nutritional and hormonal stimuli, and only *SREBP-2* responds to statins[34, 35]. Consequently, it is likely that murine studies are missing certain regulatory circuits controlled by miR-33b in the primate liver, particularly under lipogenic conditions where *SREBP-1* is induced. A role for miR-33 on FFA and TAG metabolism was first proposed by the Bommer group[11], and later confirmed by the Fernández-Hernando group[36], when they showed that genes encoding enzymes involved in fatty acid β-oxidation (*CPT1A, HADHD*, and *CROT*) and insulin signaling (*IRS2, PRKAA1*, and *SIRT6*) are functional targets of miR-33 in primates, rodents, and flies. From these studies it was inferred that miR-33 might function to limit fatty acid synthesis and utilization in the hepatocyte. More recently, the gluconeogenic genes *PCK1* and *G6PC* have also been reported as functional targets of miR-33a/b[37]. Collectively, these studies show miR-33 as a regulatory hub for multiple intracellular metabolic processes, coordinating the expression of genes involved in sterol, fatty acid, and glucose homeostasis.

The potential therapeutic use of anti-miR-33 oligonucleotides in patients at risk of developing cardiovascular disease was proposed following murine studies that showed increased circulating HDL-cholesterol[8-10], bile secretion[13], and mobilization of sterols through the RCT pathway[13, 14], compared to control oligonucleotides. The impact of ablation/reduction of miR-33 levels on atherogenesis has been evaluated in several studies using atherosclerosis-prone mouse models. The Moore group showed that a 4-week treatment with 2'-fluoro/methoxyethyl (2'F/MOE) anti-miR-33 oligonucleotides following 14-weeks of western diet (WD) feeding increased plasma HDL-cholesterol and accelerated the *regression* of atheromata. In contrast, using locked nucleic acid (LNA) oligonucleotides we showed that anti-miR-33 therapy failed to sustain elevated plasma HDL-cholesterol levels over the course of 12 weeks, raised the levels of plasma VLDL-TAG, and did not prevent the *progression* of atherosclerosis in WD-fed mice. Finally, the Fernandez-Hernando group also reported a *progression* study in which 2'F/MOE anti-miR-33 oligonucleotides did not sustain elevated plasma HDL-cholesterol, yet they led to a significant reduction in atheromata without changes in plasma TAG. The reasons behind the different outcomes among these studies remain to be elucidated, but it is possible that different bioavailability and/or potency of 2'F/MOE and LNA oligonucleotides, length of treatment, and interactions with dietary components might explain the discrepancies in HDL, VLDL and atherogenesis. Finally, ApoE$^{-/-}$ × miR-33$^{-/-}$ mice, but not ApoE$^{-/-}$ mice transplanted with miR-33$^{-/-}$ bone marrow, had decreased atherosclerotic lesions compared to ApoE$^{-/-}$ mice[38]. These latter studies imply that increased hepatic HDL biogenesis (or

perhaps bile secretion), rather than accelerated macrophage cholesterol efflux, could mediate atheroprotection following whole-body loss of miR-33. However, and paradoxically, the two progression studies that used antisense oligonucleotides in *Ldlr*$^{-/-}$ mice reported no changes in plasma HDL-cholesterol among the different treatments, despite elevated hepatic ABCA1 expression in anti-miR-33-treated mice[18, 19]. Furthermore, while this manuscript was under revision, Horie *et al*. reported that miR-33$^{-/-}$ mice developed hepatosteatosis when fed a high fat diet, but not regular chow, compared to wild-type animals[39]. These authors reasoned that *de novo* lipogenesis was induced in the knock-out mice via direct de-repression of *Srebp-1*, which was presented as a direct miR-33 target. However, the expression of key lipogenic genes (i.e. *Fasn*, *Acc1*) was identical in chow-fed wild-type and miR-33$^{-/-}$mice, complicating the interpretation of the data. In contrast to this latter study, herein we report no changes in the lipogenic ability of mouse primary hepatocytes following miR-33 overexpression. We had also reported that the potential miR-33 sequences present in the 3'-UTR of the mouse *Srebp1* did not confer responsiveness to the miRNA in our hands[13], and *Srebp1c* or *-1a* were not enriched in our RISC pull-downs following miR-33 overexpression (data not shown). Incidentally, Hori *et al*. did not note changes in plasma TAG in miR-33$^{-/-}$, compared to wild-type animals, although the values reported were abnormally low and, surprisingly, decreased in high-fat diet vs. chow (~20 vs. ~35 mg/dL, respectively)[39]. The reasons behind the discrepancies between the sustained miR-33 silencing (via oligonucleotides) and the miR-33$^{-/-}$models regarding plasma TAG and HDL-cholesterol remain obscure. Besides potential differences in the genetic backgrounds between these animals, a critical distinction is that treatment with antisense oligonucleotides results in only the partial de-repression of hepatic miR-33 targets, while the expression of miR-33 and miR-33 targets remains unchanged in metabolically relevant extrahepatic tissues (i.e., skeletal muscle, heart, adipose, and intestine); conversely, the knock-out model leads to the abolition of miR-33 and the complete de-repression of miR-33 targets in all tissues. The relative contribution of extra-hepatic miR-33 to whole-body lipid homeostasis remains to be determined, but it is conceivable that the anti-miR-33 treatment can only partially recapitulate the effects of genetic loss of miR-33. In any case, whether anti-miR-33 therapy will be effective to manage dyslipidemic patients remains an open question that will need further validation.

The Moore and Temel groups[15], and the Näär group[16] reported two independent studies in African green monkeys that showed the expected raise in HDL-cholesterol following anti-miR-33 therapy with either no change in plasma TAG[16] or lowered VLDL-TAG[15], compared to vehicle or control oligonucleotides, respectively. The analysis of VLDL metabolism in these and other non-human primates, however, is complicated by the fact that the levels of plasma TAG are only 15–30% of those in humans[24, 40-42], likely due to the very efficient clearance from circulation by lipoprotein lipase[40, 43]. Indeed, the efficiency of clearance is so high in these animals that interventions that alter hepatic VLDL secretion are difficult to detect by simply measuring plasma concentrations of TAG[43]. In the Moore and Temel study[15], VLDL-TAG represented ~25% of the total TAG in chow-fed monkeys, independent of treatment, consistent with a rapid VLDL turnover in these animals. Over time, VLDL-TAG levels increased in their control oligonucleotide group (both on chow and after switching to a moderate-cholesterol, high-carbohydrate diet) while they remained flat

in the anti-miR-33 group. This was interpreted as a *lowering effect* of the anti-miR, compared to the control oligonucleotides. An alternative interpretation is that the control oligonucleotides *raised* VLDL-TAG, compared to the anti-miR treatment. The absence of a third group of animals injected with saline precludes distinguishing between those two possibilities. Whether the Rayner control oligonucleotide alters the hepatic or peripheral expression of genes involved in VLDL-TAG metabolism or clearance is unknown, though. On the other hand, the Näär study[16] presents data from animals fed a high-fat diet, then switched to a high-carbohydrate diet, but no TAG lipoprotein distribution is shown. In any case, further studies will be necessary to establish a role for miR-33 on hepatic VLDL-TAG secretion and/or clearance in primates.

The assembly of secretion-competent VLDL particles was originally regarded as a two-step process ignited by the MTTP-dependent co-translational lipidation of APOB as it is translocated across the ER membrane, then followed by addition of lipid-droplet-derived bulk TAG within the ER and/or Golgi lumen. Recent studies in patients with inherited dyslipidemias and in mouse models have identified several additional factors involved in VLDL assembly, maturation, trafficking, degradation, and secretion[1, 2, 44-46]. The exact molecular mechanisms that control the ultimate fate of nascent VLDL-containing vesicles (secretion vs. degradation) in response to different nutritional and hormonal stimuli are not completely understood, but it is likely that these vesicles are decorated with distinct proteins that define their proper intracellular trafficking[47, 48]. As mentioned in the Introduction, specific v-SNARE (SEC22B) and t-SNAREs (STX5, BET1, and GOSR1) are required for the mobilization of APOB-containing cargo from ER to Golgi, but not for other ER-derived secretory vesicles[3, 4]. Interestingly, SEC22B has been reported to bind directly to APOB100[3]. NSF activity is required for the resolution of the SNARE complexes formed before/during vesicular membrane fusion, thus allowing the recycling of v- and t-SNAREs[6]. It is then perhaps not surprising that altered NSF expression results in changes in APOB and TAG secretion, as described in this report. It is unclear which specific steps during VLDL trafficking are directly impacted by NSF: ER to Golgi, fusion with lipid droplets, mobilization through the Golgi, and/or fusion with plasma membrane and release of the cargo. Since all these steps are SNARE-dependent, it is tempting to speculate that NSF likely modulates all trafficking aspects of intracellular VLDL mobilization. Further studies should provide clues into the consequences of deregulated NSF expression on the intracellular fate of nascent VLDL, and whether small molecules that alter NSF activity might be useful to control VLDL secretion and/or manage dyslipidemic patients. In a broader sense, the data presented herein suggest that long-term therapeutic silencing of miR-33 may result in the profound deregulation of hepatic secretion. Nevertheless, such an increase in not only pro-atherogenic VLDL but also other liver-derived circulating proteins (e.g. coagulation factors) might result in unanticipated side effects. Hence, caution should be taken with the implementation of potential anti-miR-33–based therapies.

Supplementary Material

Refer to Web version on PubMed Central for supplementary material.

Acknowledgments

We thank Erin Touchette for outstanding technical support with in vivo experiments.

SOURCES OF FUNDING

This work was supported in part by NIH Grant HL107794 (to Á.B.) and American Heart Association Predoctoral Fellowship 11PRE7240026 (to R.M.A.).

References

1. Tiwari S, Siddiqi SA. Intracellular trafficking and secretion of VLDL. Arterioscler Thromb Vasc Biol. 2012; 32:1079–1086. [PubMed: 22517366]
2. Sundaram M, Yao Z. Recent progress in understanding protein and lipid factors affecting hepatic VLDL assembly and secretion. Nutr Metab (Lond). 2010; 7:35. [PubMed: 20423497]
3. Siddiqi S, Mani AM, Siddiqi SA. The identification of the SNARE complex required for the fusion of VLDL-transport vesicle with hepatic cis-Golgi. Biochem J. 2010; 429:391–401. [PubMed: 20450495]
4. Siddiqi SA. VLDL exits from the endoplasmic reticulum in a specialized vesicle, the VLDL transport vesicle, in rat primary hepatocytes. Biochem J. 2008; 413:333–342. [PubMed: 18397176]
5. Gusarova V, Brodsky JL, Fisher EA. Apolipoprotein B100 exit from the endoplasmic reticulum (ER) is COPII-dependent, and its lipidation to very low density lipoprotein occurs post-ER. J Biol Chem. 2003; 278:48051–48058. [PubMed: 12960170]
6. Zhao C, Smith EC, Whiteheart SW. Requirements for the catalytic cycle of the N-ethylmaleimide-sensitive factor (NSF). Biochim Biophys Acta. 2012; 1823:159–171. [PubMed: 21689688]
7. Bartel DP. MicroRNAs: Target recognition and regulatory functions. Cell. 2009; 136:215–233. [PubMed: 19167326]
8. Najafi-Shoushtari SH, Kristo F, Li Y, Shioda T, Cohen DE, Gerszten RE, Naar AM. MicroRNA-33 and the SREBP host genes cooperate to control cholesterol homeostasis. Science. 2010; 238:1566–1569. [PubMed: 20466882]
9. Rayner KJ, Suarez Y, Davalos A, Parathath S, Fitzgerald ML, Tamehiro N, Fisher EA, Moore KJ, Fernandez-Hernando C. MiR-33 contributes to the regulation of cholesterol homeostasis. Science. 2010; 238:1570–1573. [PubMed: 20466885]
10. Marquart TJ, Allen RM, Ory DS, Baldan A. MiR-33 links SREBP-2 induction to repression of sterol transporters. Proc Natl Acad Sci U S A. 2010; 107:12228–12232. [PubMed: 20566875]
11. Gerin I, Clerbaux LA, Haumont O, Lanthier N, Das AK, Burant CF, Leclercq IA, MacDougald OA, Bommer GT. Expression of miR-33 from an SREBP2 intron inhibits cholesterol export and fatty acid oxidation. J Biol Chem. 2010; 285:33652–33661. [PubMed: 20732877]
12. Horie T, Ono K, Horiguchi M, Nishi H, Nakamura T, Nagao K, Kinoshita M, Kuwabara Y, Marusawa H, Iwanaga Y, Hasegawa K, Yokode M, Kimura T, Kita T. MicroRNA-33 encoded by an intron of sterol regulatory element-binding protein 2 (SREBP2) regulates HDL in vivo. Proc Natl Acad Sci U S A. 2010; 107:17321–17326. [PubMed: 20855588]
13. Allen RM, Marquart TJ, Albert CJ, Suchy FJ, Wang DQ, Ananthanarayanan M, Ford DA, Baldan A. MiR-33 controls the expression of biliary transporters, and mediates statin- and diet-induced hepatotoxicity. EMBO Mol Med. 2012; 4:882–895. [PubMed: 22767443]
14. Rayner KJ, Sheedy FJ, Esau CC, Hussain FN, Temel RE, Parathath S, van Gils JM, Rayner AJ, Chang AN, Suarez Y, Fernandez-Hernando C, Fisher EA, Moore KJ. Antagonism of miR-33 in mice promotes reverse cholesterol transport and regression of atherosclerosis. J Clin Invest. 2011; 121:2921–2931. [PubMed: 21646721]
15. Rayner KJ, Esau CC, Hussain FN, McDaniel AL, Marshall SM, van Gils JM, Ray TD, Sheedy FJ, Goedeke L, Liu X, Khatsenko OG, Kaimal V, Lees CJ, Fernandez-Hernando C, Fisher EA, Temel RE, Moore KJ. Inhibition of miR-33a/b in non-human primates raises plasma HDL and lowers VLDL triglycerides. Nature. 2011; 478:404–407. [PubMed: 22012398]
16. Rottiers V, Obad S, Petri A, McGarrah R, Lindholm MW, Black JC, Sinha S, Goody RJ, Lawrence MS, Delemos AS, Hansen HF, Whittaker S, Henry S, Brookes R, Najafi-Shoushtari SH, Chung

RT, Whetstine JR, Gerszten RE, Kauppinen S, Naar AM. Pharmacological inhibition of a microRNA family in nonhuman primates by a seed-targeting 8-mer antimiR. Sci Transl Med. 2013; 5:212ra162.

17. Rader DJ, Tall AR. The not-so-simple HDL story: Is it time to revise the HDL cholesterol hypothesis? Nat Med. 2012; 18:1344–1346. [PubMed: 22961164]
18. Rotllan N, Ramirez CM, Aryal B, Esau CC, Fernandez-Hernando C. Therapeutic silencing of microRNA-33 inhibits the progression of atherosclerosis in LDLR-/- mice--brief report. Arterioscler Thromb Vasc Biol. 2013; 33:1973–1977. [PubMed: 23702658]
19. Marquart TJ, Wu J, Lusis AJ, Baldan A. Anti-miR-33 therapy does not alter the progression of atherosclerosis in low-density lipoprotein receptor-deficient mice. Arterioscler Thromb Vasc Biol. 2013; 33:455–458. [PubMed: 23288159]
20. Olofsson SO, Boren J. Apolipoprotein B secretory regulation by degradation. Arterioscler Thromb Vasc Biol. 2012; 32:1334–1338. [PubMed: 22592119]
21. Meex SJ, Andreo U, Sparks JD, Fisher EA. HuH-7 or HepG2 cells: Which is the better model for studying human apolipoprotein-B100 assembly and secretion? J Lipid Res. 2011; 52:152–158. [PubMed: 20956548]
22. Go AS, Mozaffarian D, Roger VL, Benjamin EJ, Berry JD, Borden WB, Bravata DM, Dai S, Ford ES, Fox CS, Franco S, Fullerton HJ, Gillespie C, Hailpern SM, Heit JA, Howard VJ, Huffman MD, Kissela BM, Kittner SJ, Lackland DT, Lichtman JH, Lisabeth LD, Magid D, Marcus GM, Marelli A, Matchar DB, McGuire DK, Mohler ER, Moy CS, Mussolino ME, Nichol G, Paynter NP, Schreiner PJ, Sorlie PD, Stein J, Turan TN, Virani SS, Wong ND, Woo D, Turner MB. American Heart Association Statistics C, Stroke Statistics S. Heart disease and stroke statistics--2013 update: A report from the American Heart Association. Circulation. 2013; 127:e6–e245. [PubMed: 23239837]
23. Stein EA, Lane M, Laskarzewski P. Comparison of statins in hypertriglyceridemia. Am J Cardiol. 1998; 81:66B–69B.
24. Yin W, Carballo-Jane E, McLaren DG, Mendoza VH, Gagen K, Geoghagen NS, McNamara LA, Gorski JN, Eiermann GJ, Petrov A, Wolff M, Tong X, Wilsie LC, Akiyama TE, Chen J, Thankappan A, Xue J, Ping X, Andrews G, Wickham LA, Gai CL, Trinh T, Kulick AA, Donnelly MJ, Voronin GO, Rosa R, Cumiskey AM, Bekkari K, Mitnaul LJ, Puig O, Chen F, Raubertas R, Wong PH, Hansen BC, Koblan KS, Roddy TP, Hubbard BK, Strack AM. Plasma lipid profiling across species for the identification of optimal animal models of human dyslipidemia. J Lipid Res. 2012; 53:51–65. [PubMed: 22021650]
25. Cuchel M, Schaefer EJ, Millar JS, Jones PJ, Dolnikowski GG, Vergani C, Lichtenstein AH. Lovastatin decreases de novo cholesterol synthesis and LDL apoB-100 production rates in combined-hyperlipidemic males. Arterioscler Thromb Vasc Biol. 1997; 17:1910–1917. [PubMed: 9351353]
26. Watts GF, Naoumova RP, Kelly JM, Riches FM, Croft KD, Thompson GR. Inhibition of cholesterogenesis decreases hepatic secretion of apoB-100 in normolipidemic subjects. Am J Physiol. 1997; 273:E462–470. [PubMed: 9316434]
27. Ginsberg HN, Le NA, Short MP, Ramakrishnan R, Desnick RJ. Suppression of apolipoprotein B production during treatment of cholesteryl ester storage disease with lovastatin. Implications for regulation of apolipoprotein B synthesis. J Clin Invest. 1987; 80:1692–1697. [PubMed: 3680522]
28. Watts GF, Cummings MH, Umpleby M, Quiney JR, Naoumova R, Thompson GR, Sonksen PH. Simvastatin decreases the hepatic secretion of very-low-density lipoprotein apolipoprotein B-100 in heterozygous familial hypercholesterolaemia: Pathophysiological and therapeutic implications. Eur J Clin Invest. 1995; 25:559–567. [PubMed: 7589011]
29. Arad Y, Ramakrishnan R, Ginsberg HN. Lovastatin therapy reduces low density lipoprotein apob levels in subjects with combined hyperlipidemia by reducing the production of apoB-containing lipoproteins: Implications for the pathophysiology of apoB production. J Lipid Res. 1990; 31:567–582. [PubMed: 2351867]
30. Berthold HK, Mertens J, Birnbaum J, Bramswig S, Sudhop T, Barrett PH, von Bergmann K, Gouni-Berthold I. Influence of simvastatin on apoB-100 secretion in non-obese subjects with mild hypercholesterolemia. Lipids. 2010; 45:491–500. [PubMed: 20461472]

31. Lamon-Fava S, Diffenderfer MR, Barrett PH, Buchsbaum A, Matthan NR, Lichtenstein AH, Dolnikowski GG, Horvath K, Asztalos BF, Zago V, Schaefer EJ. Effects of different doses of atorvastatin on human apolipoprotein A-100, B-48, and A-I metabolism. J Lipid Res. 2007; 48:1746–1753. [PubMed: 17526934]
32. Chan DC, Watts GF, Barrett PH, Mori TA, Beilin LJ, Redgrave TG. Mechanism of action of a 3-hydroxy-3-methylglutaryl coenzyme a reductase inhibitor on apolipoprotein B-100 kinetics in visceral obesity. J Clin Endocrinol Metab. 2002; 87:2283–2289. [PubMed: 11994377]
33. Parhofer KG, Barrett PH, Dunn J, Schonfeld G. Effect of pravastatin on metabolic parameters of apolipoprotein B in patients with mixed hyperlipoproteinemia. Clin Investig. 1993; 71:939–946.
34. Horton JD, Bashmakov Y, Shimomura I, Shimano H. Regulation of sterol regulatory element binding proteins in livers of fasted and refed mice. Proc Natl Acad Sci U S A. 1998; 95:5987–5992. [PubMed: 9600904]
35. Bennett MK, Seo YK, Datta S, Shin DJ, Osborne TF. Selective binding of sterol regulatory element-binding protein isoforms and co-regulatory proteins to promoters for lipid metabolic genes in liver. J Biol Chem. 2008; 283:15628–15637. [PubMed: 18413311]
36. Davalos A, Goedeke L, Smibert P, Ramirez CM, Warrier NP, Andreo U, Cirera-Salinas D, Rayner K, Suresh U, Pastor-Pareja JC, Esplugues E, Fisher EA, Penalva LO, Moore KJ, Suarez Y, Lai EC, Fernandez-Hernando C. MiR-33a/b contribute to the regulation of fatty acid metabolism and insulin signaling. Proc Natl Acad Sci U S A. 2011; 108:9232–9237. [PubMed: 21576456]
37. Ramirez CM, Goedeke L, Rotllan N, Yoon JH, Cirera-Salinas D, Mattison JA, Suarez Y, de Cabo R, Gorospe M, Fernandez-Hernando C. MicroRNA 33 regulates glucose metabolism. Mol Cell Biol. 2013; 33:2891–2902. [PubMed: 23716591]
38. Horie T, Baba O, Kuwabara Y, Chujo Y, Watanabe S, Kinoshita M, Horiguchi M, Nakamura T, Chonabayashi K, Hishizawa M, Hasegawa K, Kume N, Yokode M, Kita T, Kimura T, Ono K. MicroRNA-33 deficiency reduces the progression of atherosclerotic plaque in apoE−/− mice. J Am Heart Assoc. 2012; 1:e003376. [PubMed: 23316322]
39. Horie T, Nishino T, Baba O, Kuwabara Y, Nakao T, Nishiga M, Usami S, Izuhara M, Sowa N, Yahagi N, Shimano H, Matsumura S, Inoue K, Marusawa H, Nakamura T, Hasegawa K, Kume N, Yokode M, Kita T, Kimura T, Ono K. MicroRNA-33 regulates sterol regulatory element-binding protein 1 expression in mice. Nat Commun. 2013; 4:2883. [PubMed: 24300912]
40. Marzetta CA, Johnson FL, Zech LA, Foster DM, Rudel LL. Metabolic behavior of hepatic VLDL and plasma LDL apoB-100 in african green monkeys. J Lipid Res. 1989; 30:357–370. [PubMed: 2723543]
41. Parks JS, Martin JA, Sonbert BL, Bullock BC. Alteration of high density lipoprotein subfractions of nonhuman primates fed fish-oil diets. Selective lowering of HDL subfractions of intermediate size and density. Arteriosclerosis. 1987; 7:71–79. [PubMed: 3813977]
42. Parks JS, Bullock BC. Effect of fish oil versus lard diets on the chemical and physical properties of low density lipoproteins of nonhuman primates. J Lipid Res. 1987; 28:173–182. [PubMed: 3572246]
43. Parks JS, Johnson FL, Wilson MD, Rudel LL. Effect of fish oil diet on hepatic lipid metabolism in nonhuman primates: Lowering of secretion of hepatic triglyceride but not apoB. J Lipid Res. 1990; 31:455–466. [PubMed: 2341808]
44. Calandra S, Tarugi P, Speedy HE, Dean AF, Bertolini S, Shoulders CC. Mechanisms and genetic determinants regulating sterol absorption, circulating LDL levels, and sterol elimination: Implications for classification and disease risk. J Lipid Res. 2011; 52:1885–1926. [PubMed: 21862702]
45. Fisher EA. The degradation of apolipoprotein B100: Multiple opportunities to regulate VLDL triglyceride production by different proteolytic pathways. Biochim Biophys Acta. 2012; 1821:778–781. [PubMed: 22342675]
46. Haas ME, Attie AD, Biddinger SB. The regulation of apoB metabolism by insulin. Trends Endocrinol Metab. 2013; 24:391–397. [PubMed: 23721961]
47. Rahim A, Nafi-valencia E, Siddiqi S, Basha R, Runyon CC, Siddiqi SA. Proteomic analysis of the very low density lipoprotein (VLDL) transport vesicles. J Proteomics. 2012; 75:2225–2235. [PubMed: 22449872]

48. Rashid KA, Hevi S, Chen Y, Le Caherec F, Chuck SL. A proteomic approach identifies proteins in hepatocytes that bind nascent apolipoprotein B. J Biol Chem. 2002; 277:22010–22017. [PubMed: 11934886]

Nonstandard Abbreviations and Acronyms

APOA1	apoprotein A1
APOB	apoprotein B
COPII	coat complex II
HDL	high-density lipoprotein
MTTP	microsomal triacylglyceride transfer protein
NSF	N-ethylmaleimide-sensitive factor
RCT	reverse cholesterol transport
RISC	RNA-induced silencing complex
SNAP	soluble NSF-attachment protein
SNARE	vesicle-N-ethylmaleimide-sensitive factor-attachment protein receptor
TAG	triacylglycerides
VLDL	very low-density lipoprotein

Novelty and Significance

What Is Known?

- Specific microRNAs (miRNAs) fine-tune the expression of genes involved in cardiovascular health and disease.
- Short-term anti-miR-33 therapy increases plasma HDL-cholesterol and hepatic bile secretion, and accelerates reverse cholesterol transport in mice.
- The effects of anti-miR-33 therapy on atherogenesis in mice are controversial.

What New Information Does This Article Contribute?

- Anti-miR-33 oligonucleotides increase the secretion of hepatic VLDL-triglyceride in chow-fed mice.
- N-ethylmaleimide-sensitive factor (NSF) is a conserved, direct target of miR-33, and facilitates miR-33–dependent changes in secretion.
- The miR-33–NSF axis modulates the constitutive secretory pathway in the hepatocyte.

Several studies suggested that anti-miR-33 therapy might be atheroprotective. However, conflicting data has been reported on the impact of anti-miR-33 oligonucleotides on plasma triglycerides (TAG). Here we show that miR-33 controls the hepatic secretory pathway via NSF. Thus, manipulation of either miR-33 or NSF levels in both primary hepatocytes and in vivo results in profound changes in the secretion of not only VLDL-TAG, but also a plethora of liver–derived circulating proteins. In a general sense, our results reveal the risk of undesired effects following miRNA therapeutic antagonism, and highlight the need for comprehensive characterization and understanding of physiologic miRNA targets. In the case of miR-33, in vivo antagonism results in the de-repression of both anti-atherogenic pathways (previous reports) and pro-atherogenic pathways (this report). Further studies will be necessary to establish whether miR-33 is a safe therapeutic target to manage cardiovascular disease in patients.

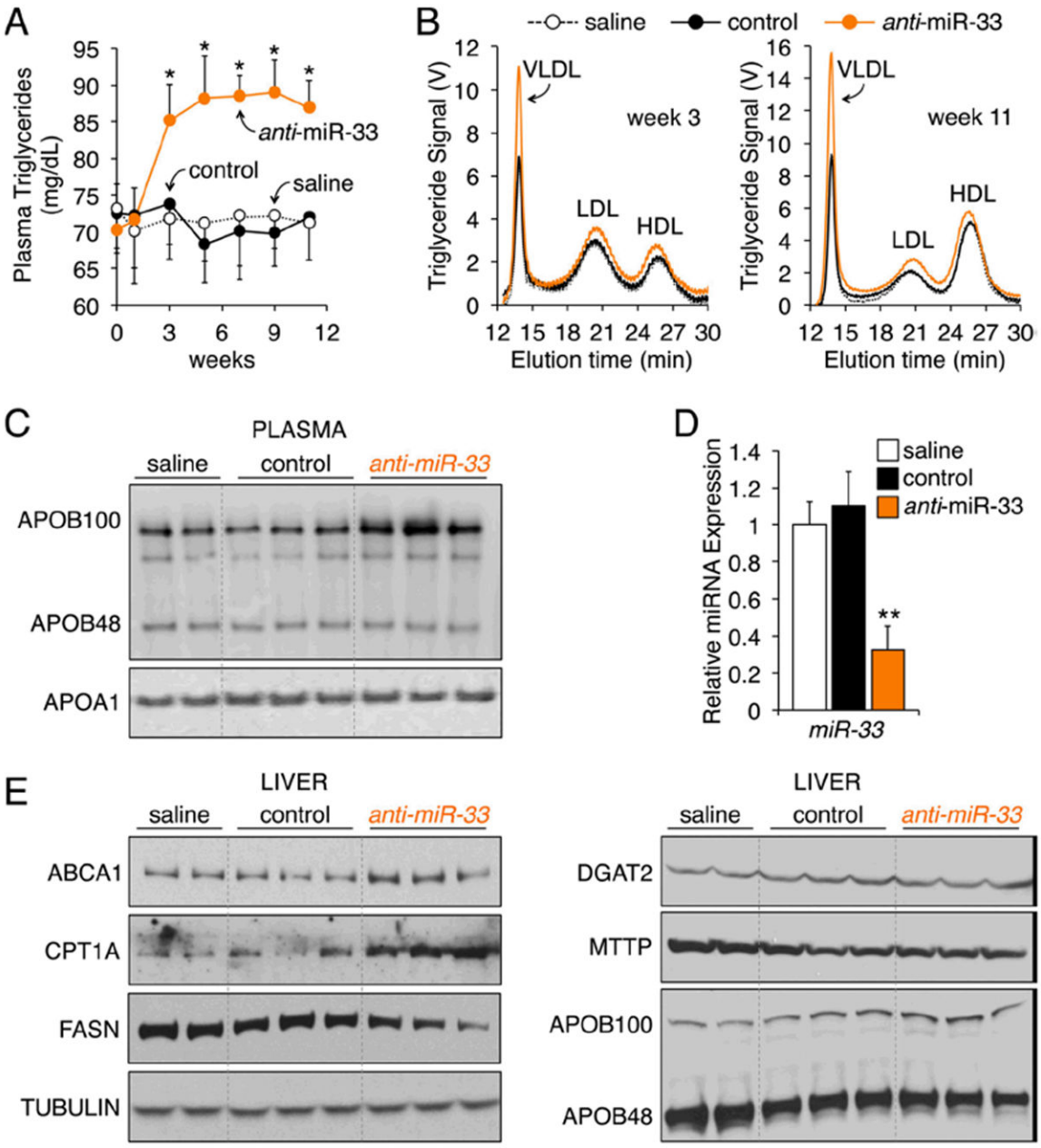

Figure 1. Silencing of miR-33 results in sustained elevation of plasma VLDL-TAG in mice

Chowfed C57BL/6 mice were injected i.p. with saline (n=5), or control (n=7) or anti-miR-33 (n=7) oligonucleotides (5 mg/Kg/week) for 11 weeks. Animals were fasted overnight before blood collection or sacrifice. (A) Plasma triglyceride levels over time. Data are mean ± SEM; **P* ≤ 0.05. (B) TAG lipoprotein profiles at weeks 3 and 11, as determined by FPLC. (C) Immunoblots for APOB and APOA1 in individual plasma samples from week 11. (D) Relative hepatic miR-33 expression at week 11. Data are mean ± SEM; ***P* ≤ 0.01. (E) Immunoblots for selected proteins in the same livers.

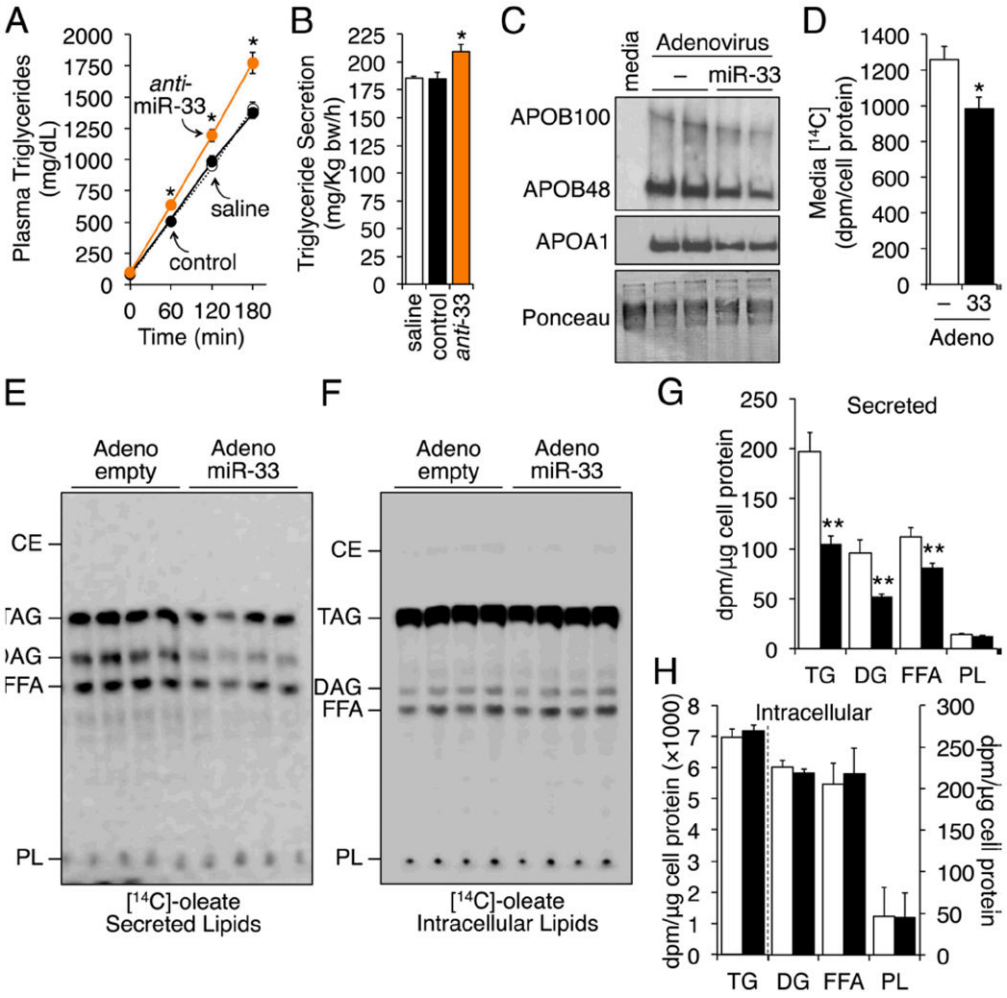

Figure 2. MiR-33 limits the secretion of VLDL in vivo and in primary hepatocytes

(A) Kinetics of plasma TAG accumulation in C57BL/6 mice (n=6/group) dosed as in Figure 1 for 6 weeks, and injected i.v. with tyloxapol (see text for details). Data are mean ± SEM; **P* ≤ 0.05. (B) Hepatic TAG secretion rates, calculated from the data above. Data are mean ± SEM; **P* ≤ 0.05. (C) Immunoblots for APOB and APOA1 in supernatants from mouse primary hepatocytes transduced with empty or miR-33 adenovirus, then pulsed in media supplemented with 0.8 mmol/L oleate. First lane contains media not incubated with cells. (D) Total radioactivity, normalized to intracellular protein, in the supernatants of mouse primary hepatocytes transduced with empty or miR-33 adenovirus, pulsed in media supplemented with 0.8 mmol/L oleate and 1 µCi/mL [^{14}C]-oleate for 16 h, and chased in fresh media for 24 h. Data are mean ± SEM of 2 independent experiments in quadruplicate. **P* ≤ 0.05. (E) Lipids were extracted from the above supernatants, resolved by TLC, and visualized with a PhosphorImager. (F) Lipids were extracted from the cells in (D), and resolved by TLC as above. (G) Spots in (E) were scraped from the silica plate, and radioactivity determined by scintillation and normalized to intracellular protein. Data are mean ± SEM. ***P* ≤ 0.01. (H) Spots in (F) were scraped from the silica plate, and radioactivity determined by scintillation and normalized to intracellular protein. Data are mean ± SEM.

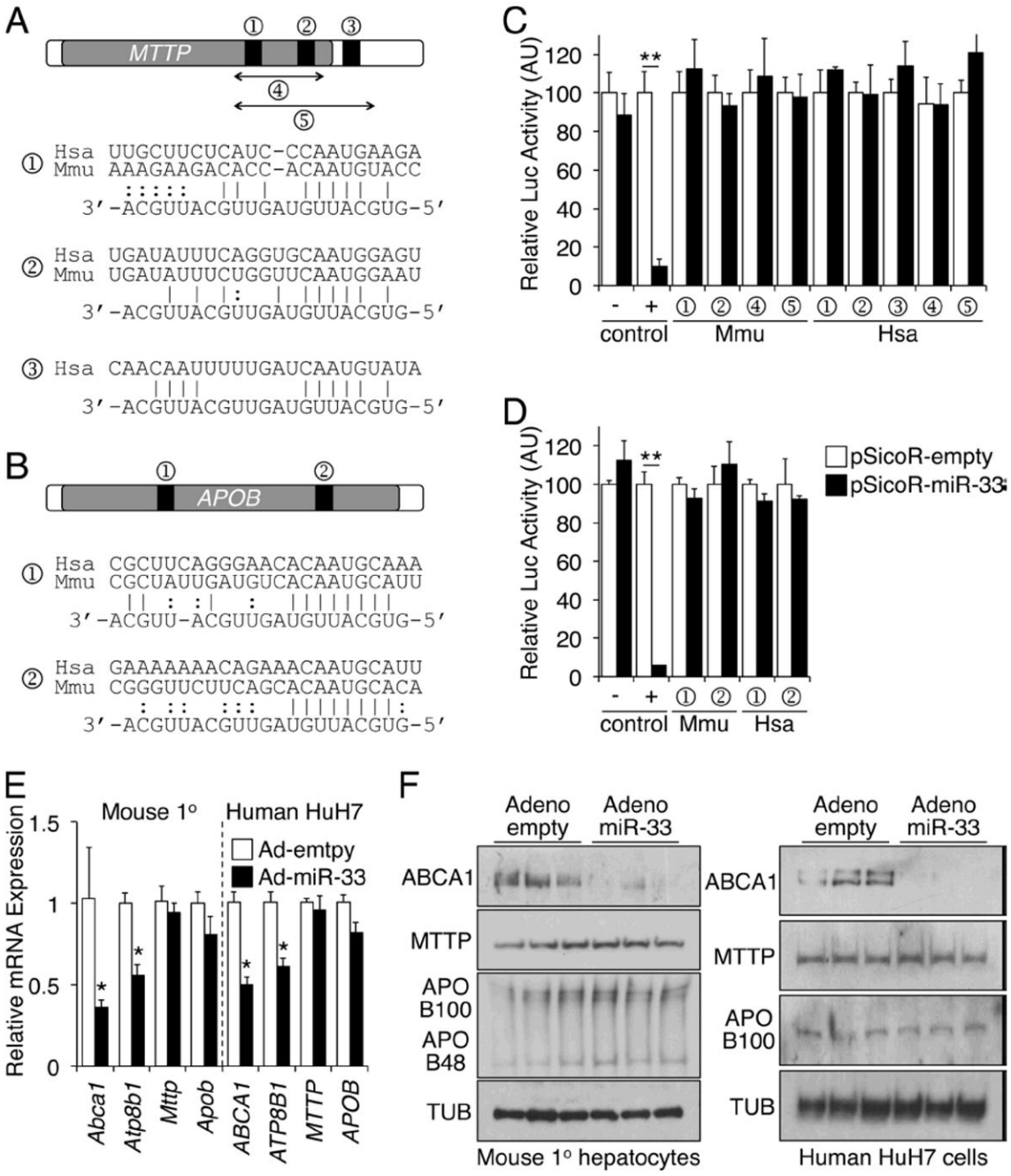

Figure 3. APOB and MTTP are not direct, functional targets of miR-33

(A) Sequences in the human (Hsa) and mouse (Mmu) coding region and 3'UTR of *MTTP* with partial complementarity to miR-33 are shown as elements 1, 2, and 3. (B) Sequences in the human (Hsa) and mouse (Mmu) coding region of *APOB* transcript with partial complementarity to miR-33 are shown as elements 1 and 2. (C) Normalized relative luciferase activity in extracts from HEK293 cells transiently transfected with a reporter fused to the potential miR-33 responsive elements identified in mouse or human *MTTP* 3'UTR, in the absence (open bars) or presence (closed bars) of an expression vector for miR-33. A positive (+) control contains a sequence that is 100% complementary to miR-33.

The negative (−) control is the empty pGL3Promoter vector. Data are mean ± SEM of 4 independent experiments in triplicate. $^{**}P \leq 0.01$. (D) Luciferase data for reporters fused to the sequence identified in *APOB* were obtained as above. (E) Relative expression of selected transcripts in mouse primary hepatocytes and Human HuH7 cells 48 h after transduction with empty or miR-33 adenovirus. Data are mean ± SEM of 3 independent experiments in triplicate. $^{*}P \leq 0.05$. (F) Immunoblots for selected proteins in extracts from cells processed in parallel.

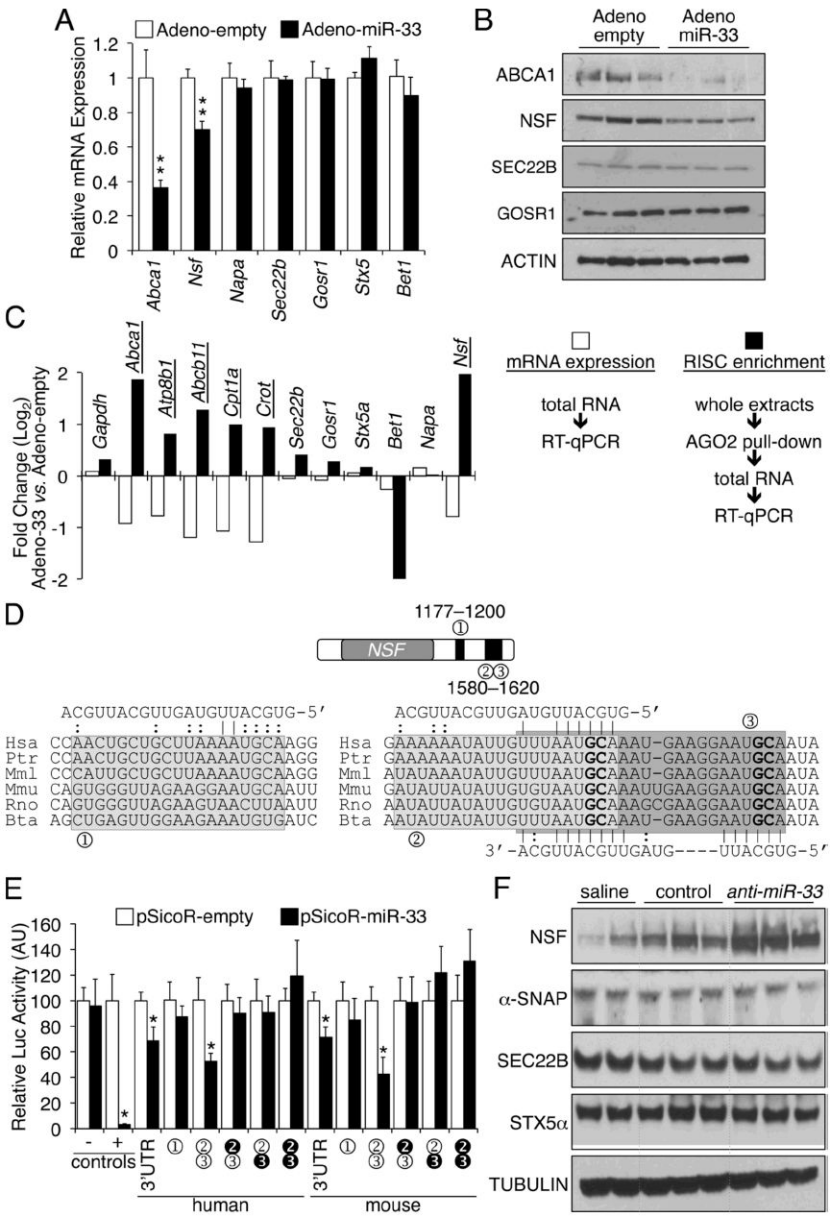

Figure 4. NSF is a direct, functional target of miR-33

(A) Relative expression of selected transcripts in mouse primary hepatocytes 48 h after transduction with empty or miR-33 adenovirus. Data are mean ± SEM of 3 independent experiments in triplicate. *$P \leq 0.05$, **$P \leq 0.01$. (B) Immunoblots for selected proteins in extracts from cells processed in parallel. (C) Relative abundance ($\log_2$) of selected transcripts in total RNA (open bars) or RNA isolated from immunoprecipated RISC (closed bars) in mouse primary hepatocytes transduced with empty or miR-33 adenovirus, as determined by RT-qPCR. Transcripts that fit the criteria of bona-fide miR-33 targets are underlined. See text for details. (D) Putative miR-33-responsive sequences in the 3'UTR of NSF (elements 1, 2, and 3) are evolutionarily conserved. Numbers indicate position after the stop codon. Elements 2 and 3 are partially overlapping. Bold nt were mutated to TT for transfection experiments below. (E) Normalized relative luciferase activity in extracts from

HEK293 cells transiently transfected with a pGL3Promoter luciferase reporter fused to the mouse or human NSF 3'UTR, or wild type (open circles) or mutant (closed circles) putative response elements described above, in the absence (open bars) or presence (closed bars) of an expression vector for miR-33. Positive (+) and negative (−) controls as described in Figure 3. Data are mean ± SEM of 4 independent experiments in triplicate. *$P \leq 0.05$. (F) Immunoblots for selected proteins in liver extracts from the same mice used in Figure 1.

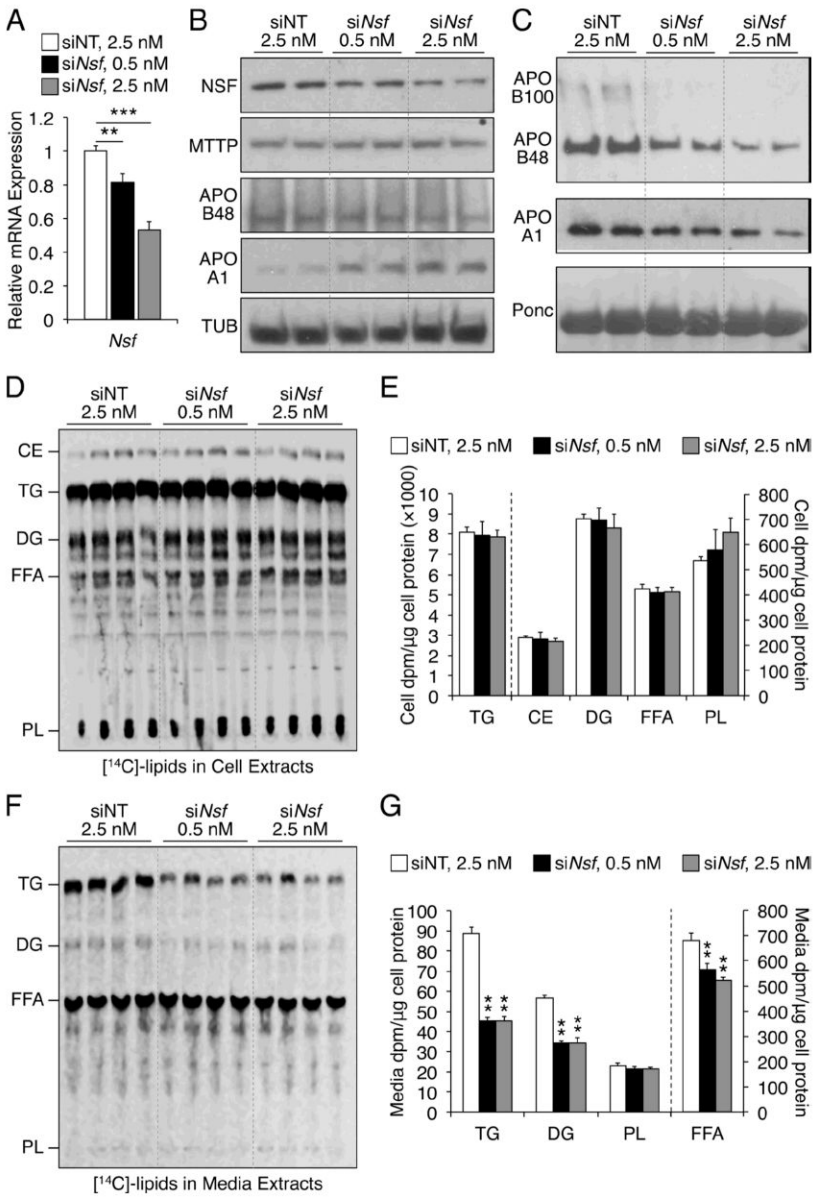

Figure 5. Partial knock-down of NSF results in decreased secretion of apoproteins and lipids in primary mouse hepatocytes

Mouse primary hepatocytes were transfected with non-targeting (siNT) or anti-NSF (si*Nsf*) siRNA oligonucleotides, pulsed 16 h in media supplemented with 0.8 mmol/L oleate and in the absence (A–C) or presence (D–G) of 1 μCi/mL [^{14}C]-oleate, then chased in fresh media for 24 h. (A) Relative mRNA levels of *Nsf*. Data are mean ± SEM; $^{**}P \leq 0.01$, $^{***}P \leq 0.001$. (B) Immunoblots for selected intracellular proteins. (C) Immunoblots for APOB and APOA1 in supernatants from the same cells. (D) Intracellular lipids were extracted from pulsed/chased cells and resolved by TLC. Labeled lipids visualized with a PhosphorImager. (E) Spots above were scraped from the silica plate, and radioactivity determined by scintillation and normalized to intracellular protein. Data are mean ± SEM. $^{**}P \leq 0.01$. (F) Lipids were extracted from the supernatants of the same cells, and resolved by TLC as

above. (G) Spots were scraped from the silica plate, and radioactivity determined by scintillation and normalized to intracellular protein. Data are mean ± SEM.

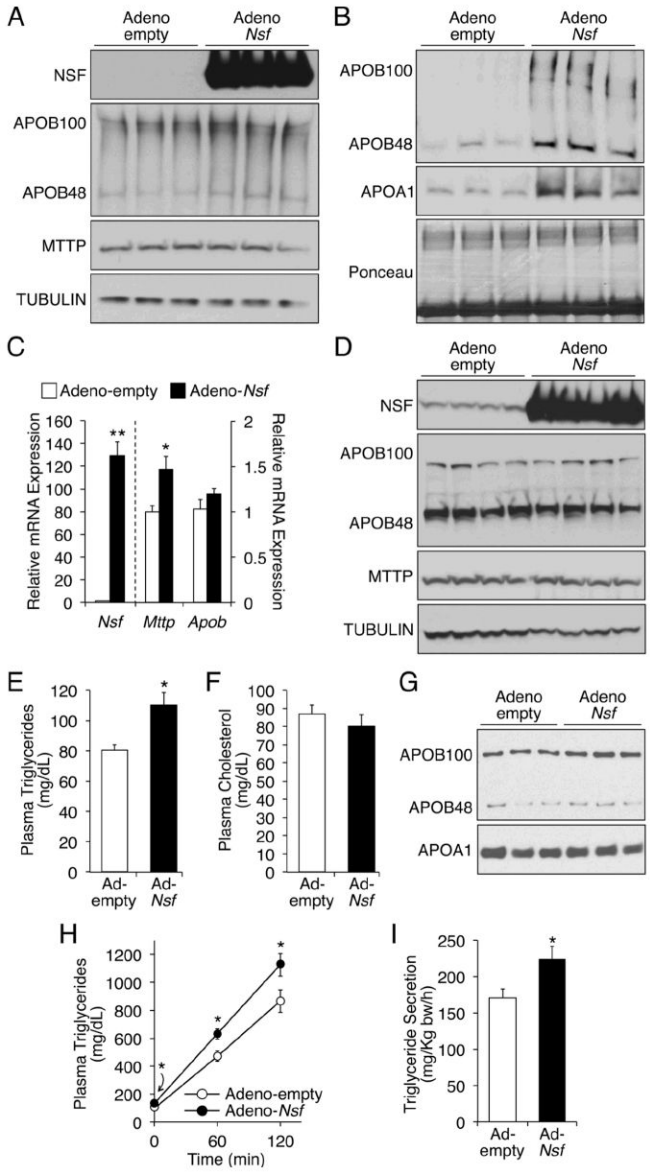

Figure 6. Exogenous overexpression of NSF accelerates VLDL secretion

(A) Immunoblots for APOB and MTTP in extracts from mouse primary hepatocytes transduced with Adeno-empty or Adeno-*Nsf* vectors. (B) Immunoblots for APOB and APOA1 in supernatants from the same cells. (C) Relative hepatic mRNA expression of selected genes in chow-fed mice 7 days after transduction with Adeno-empty of Adeno-*Nsf*, as determined by RT-qPCR. Data are mean ± SEM (n=5). *$P \leq 0.05$; **$P \leq 0.01$. (D) Immunoblots for APOB and MTTP in liver extracts from the same mice. (E) TAG lipoprotein profiles and overall contents in plasma samples from the same mice. Data are mean ± SEM (n=5). *$P \leq 0.05$. (F) Cholesterol lipoprotein profiles and overall contents in plasma samples from the same mice. Data are mean ± SEM (n=5). (G) Immunoblots for APOB and APOA1 in plasma samples from the same mice. (H) Time-dependent accumulation of plasma TAG after tyloxapol infusion in a separate group of mice 7 days after transduction with Adeno-empty of Adeno-*Nsf*. Data are mean ± SEM (n=6). *$P \leq 0.05$.

(I) Hepatic TAG secretion rates calculated from the data in (H). Data are mean ± SEM (n=6). *$P \leq 0.05$.

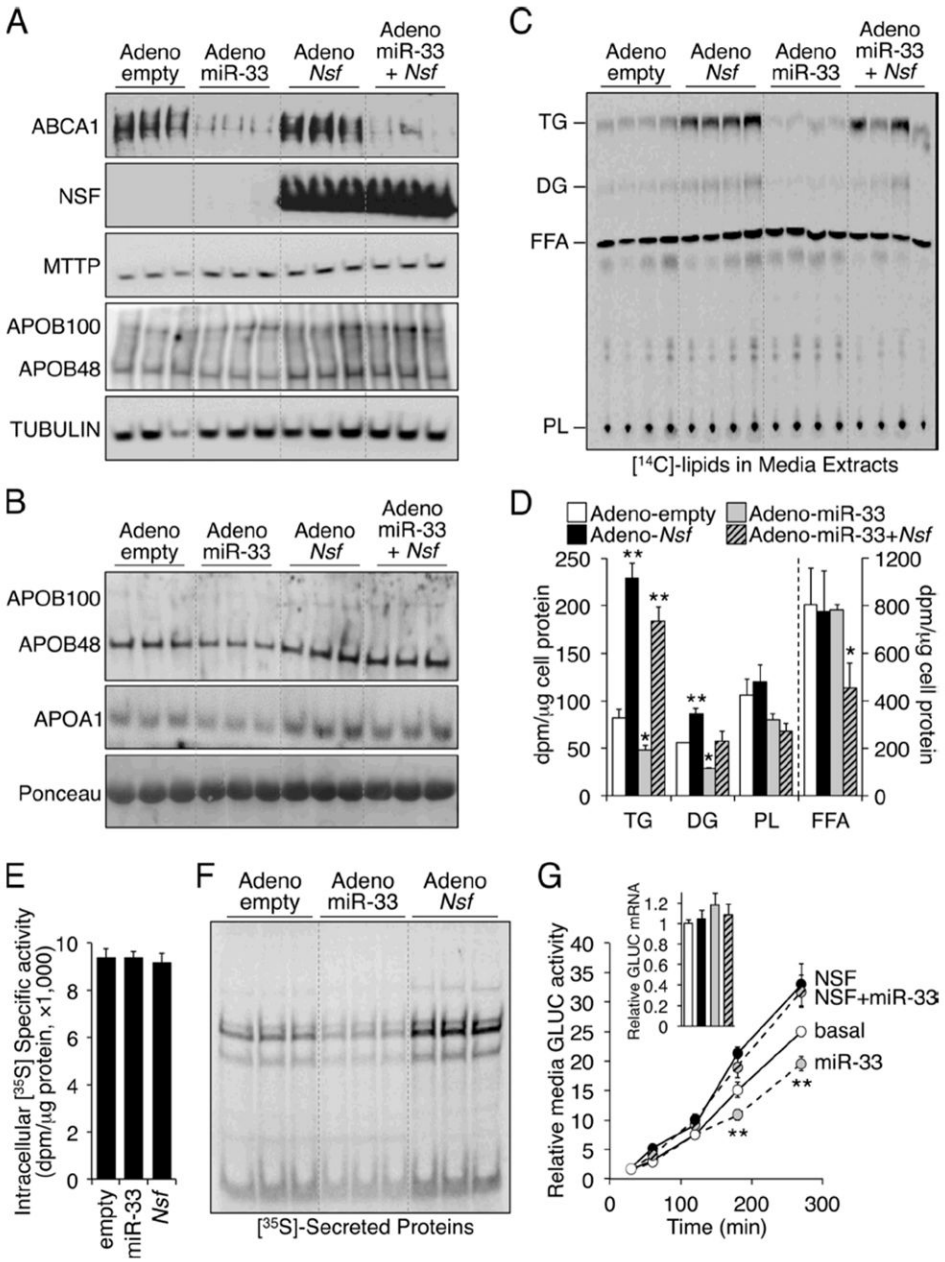

Figure 7. NSF Rescues miR-33–dependent Changes in Secretion

Mouse Primary hepatocytes were transduced with empty, miR-33, and/or *Nsf* adenovirus, as indicated. Cells were pulsed 16 h in media supplemented with 0.8 mmol/L oleate and in the absence (A, B) or presence (C, D) of 1 μCi/mL [^{14}C]-oleate, then chased in fresh media for 24 h. A different set of cells (E, F) was pulsed 30 min with 200 μCi/mL [^{35}S]-Met/Cys and chased for 3 h. (A) Immunoblots for selected intracellular proteins. (B) Immunoblots for APOB and APOA1 in supernatants from the same cells. (C) Lipids were extracted from the supernatants of [^{14}C] pulsed/chased cells and resolved by TLC. Labeled lipids visualized with a PhosphorImager. (D) Spots above were scraped from the silica plate, and radioactivity determined by scintillation and normalized to intracellular protein. Data are

mean ± SEM. *$P \leq 0.05$; **$P \leq 0.01$. (E) Specific activity of protein extracts recovered from [^{35}S]-Met/Cys pulsed/chased cells. Data are mean ± SEM of 2 independent experiments in triplicate. (F) Autoradiography of supernatants recovered from the same cells and resolved by electrophoresis. (G) Time course of GLUC activity in the media, normalized to intracellular LUC activity, from HuH7 cells transiently transfected with expression vectors for miR-33 and/or NSF. Insert shows relative *Gluc* mRNA levels in cells transfected in parallel. Data are mean ± SEM of 4 independent experiments in quintuplicate. **$P \leq 0.01$.

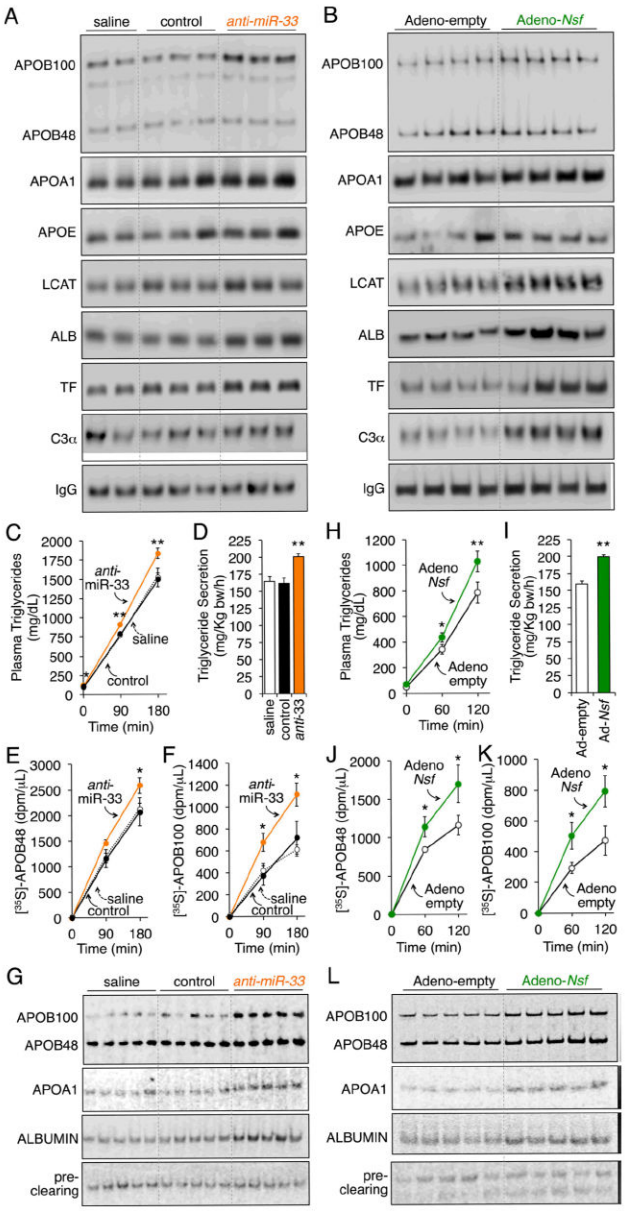

Figure 8. The miR-33–NSF Axis Controls Global Secretion

(A) Immunoblots for proteins of interest in plasma samples from mice dosed weekly with saline, or 5 mg/Kg control or anti-miR-33 oligonucleotides for 24 weeks. (B) Immunoblots for proteins of interest in plasma samples from mice infused with an empty adenovirus or and adenovirus encoding *Nsf*. (C–G) C57BL/6 mice (n=6/group) were dosed weekly with saline, or 5 mg/Kg control or anti-miR-33 oligonucleotides for 6 weeks, fasted for 4 h, and injected i.v. with 500 μCi [^{35}S]-Met/Cys and 500 mg/Kg tyloxapol. (C) Kinetics of plasma TAG accumulation. (D) Hepatic TAG secretion rates, calculated from the data above. (E, F) APOB48/100 were immunoprecipitated from 10 μL of plasma, resolved by electrophoresis, excised from the gel, and the amount of radioactivity determined by scintillation. Panels show the time-dependent accumulation of newly-synthetized circulating APOB48 and APOB100. (G) Specific proteins were immunoprecipitated from 10 μL of plasma, resolved

by electrophoresis, and exposed to a PhosphorImager screen to determine the relative [^{35}S] contents. (H–L) C57BL/6 mice (n=6/group) were infused with and empty adenovirus or an adenovirus encoding *Nsf*, and after 7 days fasted for 4 h, and injected i.v. with 500 μCi [^{35}S]-Met/Cys and 500 mg/Kg tyloxapol. Samples were processed as described above. Data are mean ± SEM. *$P \leq 0.05$; **$P \leq 0.01$.